

UC Irvine

UC Irvine Previously Published Works

Title

Oceanic uptake and the global atmospheric acetone budget

Permalink

<https://escholarship.org/uc/item/4xk0c8c1>

Journal

Geophysical Research Letters, 32(15)

ISSN

0094-8276

Authors

Marandino, C. A.
De Bruyn, W. J.
Miller, S. D.
[et al.](#)

Publication Date

2005-08-01

DOI

10.1029/2005GL023285

Supplemental Material

<https://escholarship.org/uc/item/4xk0c8c1#supplemental>

Copyright Information

This work is made available under the terms of a Creative Commons Attribution License, available at <https://creativecommons.org/licenses/by/4.0/>

Peer reviewed

Oceanic uptake and the global atmospheric acetone budget

C. A. Marandino,¹ W. J. De Bruyn,² S. D. Miller,¹ M. J. Prather,¹ and E. S. Saltzman¹

Received 19 April 2005; revised 25 May 2005; accepted 29 June 2005; published 9 August 2005.

[1] In this study, direct measurements of the air/sea flux of acetone were made over the North Pacific Ocean. The results demonstrate that the net flux of acetone is into, rather than out of the oceans. The extrapolated global ocean uptake of 48 Tg yr⁻¹ requires a major revision of the atmospheric acetone budget. This result is consistent with a recent reevaluation of acetone photodissociation quantum yields. **Citation:** Marandino, C. A., W. J. De Bruyn, S. D. Miller, M. J. Prather, and E. S. Saltzman (2005), Oceanic uptake and the global atmospheric acetone budget, *Geophys. Res. Lett.*, 32, L15806, doi:10.1029/2005GL023285.

1. Introduction

[2] Ozone photolysis and the reaction of O(¹D) with water vapor is the major tropospheric source of hydroxyl (OH) radical. In the drier upper troposphere, oxygenated organic compounds, like acetone, are major sources of HO_x (OH and HO₂). Field campaigns have shown that acetone concentrations in the upper troposphere account for about a third of the OH production, an order of magnitude higher HO_x production rate than the O(¹D) reaction with water vapor, and up to half of the observed peroxyacetyl nitrate (PAN) [Singh *et al.*, 1995; Wennberg *et al.*, 1998]. Understanding the global acetone budget and the origin of upper tropospheric acetone is important for modeling the reactivity of this portion of the atmosphere. The sources of acetone include anthropogenic emissions, biomass burning, terrestrial vegetation, plant decay, and the oxidation of isoalkanes, monoterpenes, and methylbutenol [Singh *et al.*, 1994, 2000; Brasseur *et al.*, 1998; Wang *et al.*, 1998; Collins *et al.*, 1999]. A large ocean source was inferred from aircraft measurements of acetone concentrations over the remote Pacific Ocean [Singh *et al.*, 2001], but this has been called into question by recent measurements showing depletion of acetone in the Pacific marine boundary layer relative to the overlying free troposphere [Singh *et al.*, 2003]. Previous budgets have ranged widely in the ocean's role, varying from a 21 Tg yr⁻¹ source [Jacob *et al.*, 2002] to a 14 Tg yr⁻¹ sink [Singh *et al.*, 2004]. Acetone can be produced in surface waters by the solar irradiation of dissolved organic matter [Kieber *et al.*, 1990; Zhou and Mopper, 1997] and by microbial metabolism [Nemecek-Marshall *et al.*, 1995]. There have been limited observations of acetone in oceanic waters [Zhou and Mopper, 1997; Williams *et al.*, 2004] and the only direct flux measurements of acetone have been over land [Shaw *et al.*, 1998]. Here we report direct flux

measurements indicating that the sea surface is a major sink rather than a source of atmospheric acetone. These observations imply that the global acetone budget needs to be revised, supporting a recent downward revision of the quantum yields for acetone photodissociation [Blitz *et al.*, 2004].

2. Methods

[3] Shipboard measurements of acetone in water and air were made in the Pacific Ocean during May–July 2004. The cruise track extended southeastward from Guam through the Pacific warm pool, then eastward in equatorial waters to 165°W, then northward to 40°N. Acetone measurements were made at >1 Hz frequency using atmospheric pressure chemical ionization mass spectrometry (API-CIMS) [Eisele, 1986; Viggiano *et al.*, 1988; Bandy *et al.*, 2002] with detection of protonated acetone at mass 59. Air was sampled from the bow mast at 10m height through 250 feet of 3/8" ID Teflon tubing at 27 slpm. Simultaneous measurements of 3D winds and platform angular rates and accelerations were made to allow calculation of air/sea flux by eddy covariance [Edson *et al.*, 1998]. Flux measurements are reported for relative winds within ±60° of the bow. Seawater acetone levels were determined by analyzing an air stream continuously equilibrated with seawater pumped from the bow at a depth of 5m. The measurement protocol consisted of alternating measurements of seawater (10 minute) and air (60 minutes). The instrument response was calibrated twice daily by addition of a gas standard to air and equilibrated seawater samples (S/N for a 500 ppt signal is 70 at 1 Hz). Flux was determined by integrating the cospectrum of fluctuations of the vertical wind and atmospheric acetone mixing ratio [Lenschow, 1995]. The lag between DMS and winds was determined by optimizing the covariance in a time window about the measured delay (12s). The low frequency portion of the cospectrum (<0.005 Hz) was removed to eliminate features due to undersampling. The acetone flux was corrected for high frequency attenuation in the inlet tubing based on a comparison to the frequency dependence of the temperature flux. This correction was approximately 25% and did not change the sign of the flux. The overall uncertainty in the flux due to low and high frequency corrections and motion correction is estimated to be 30–40% [Edson *et al.*, 1998; Sakai *et al.*, 2001]. The cospectra exhibit the typical frequency dependence associated with scalar surface fluxes (Figure 1) [Kaimal *et al.*, 1972], indicating that we successfully measured gas flux due to turbulent atmospheric motions. An analogous cospectrum for temperature, measured using the sonic anemometer, is shown for comparison.

[4] Acetone is believed to dominate the API-CIMS signal at mass 59 [Williams *et al.*, 2000, 2001], however there are several other oxygenated hydrocarbons whose

¹Department of Earth System Science, University of California, Irvine, California, USA.

²Department of Physical Sciences, Chapman University, Orange, California, USA.

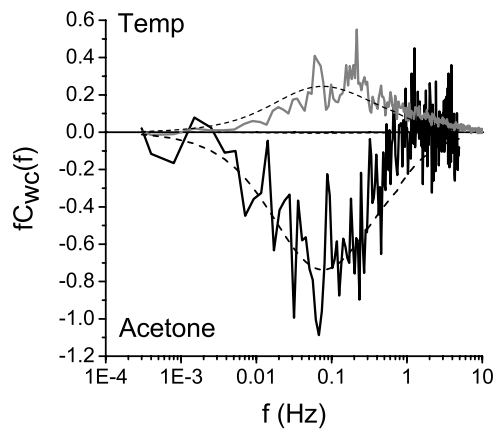


Figure 1. Frequency-weighted cospectra of scalar and vertical wind ($w'c'$) for an hour long record of temperature and acetone at 29°N, 154°W on June 24, 2004. Dashed lines are scalar cospectra from *Kaimal et al.* [1972]. The w-temperature cospectrum and Kaimal cospectra were scaled for comparison.

parent ions are at this mass. Of these, propanal is perhaps the most likely potential interferent, with an instrument response ratio of approximately 0.8 relative to acetone under the conditions used in this study. The interference from propanal is believed to be minor because the atmospheric levels are low and the flux is believed to be out of the ocean [*Singh et al.*, 2003]. However, the accuracy of the current database of atmospheric aldehyde measurements is uncertain due to the potential for artifacts during sample collection [*Apel et al.*, 2003]. Until this issue is resolved, the measurements presented here represent upper limits on the acetone concentration.

3. Results and Discussion

[5] In the western tropical Pacific Ocean, atmospheric acetone levels were 0.361 ± 0.051 (1σ) ppb (Figure 2). During this period of the cruise, air mass back-trajectories show consistent easterly trade wind flow over equatorial waters. These levels are similar to boundary layer aircraft measurements of approximately 0.400 ppb, previously reported for this region [*Singh et al.*, 2001]. Acetone levels were markedly higher northward of 25°N, with a mean of 1.04 ± 0.33 ppb, reflecting continental influence. Air mass back-trajectories and chemical tracers suggest that some of the spikes in acetone observed during this period were caused by biomass burning sources over the NW Canada and Alaska.

[6] Acetone levels in seawater exhibited a different pattern of variability than the atmosphere (Figure 2). In the tropical waters, seawater acetone concentrations were 0.54 ± 0.46 ppb (14.5 ± 12.7 nM). Seawater acetone in this region was more variable and, on average, higher than the atmospheric levels. Northward of 25°N, the mean ocean level of acetone was 0.36 ± 0.11 ppb (12.1 ± 3.0 nM). In this region, the seawater acetone concentrations were lower than those of the overlying atmosphere. The seawater concentrations of acetone measured in this study are similar to those reported previously, approximately 3 and 18 nM [*Zhou and Mopper*, 1997; *Williams et al.*, 2004].

[7] The observed saturation state is expressed as the measured water concentration in mol m^{-3} air divided by the measured air concentration in mol m^{-3} air, C_w/C_a . C_w is the gas phase concentration at equilibrium with the seawater acetone concentration, calculated by dividing molarity by the Henry's law solubility [*Zhou and Mopper*, 1990]. In the equatorial region the saturation state ranged from about 0.35 to 6.5 (Figure 2), suggesting that both positive and negative fluxes should have been observed. Surprisingly, all of the acetone fluxes measured by eddy covariance in this study were negative, illustrating that the air/sea flux is uniformly into, rather than out of the ocean. The eddy covariance fluxes suggest that the measured saturation states do not reflect the true gradient at the air/sea interface. To illustrate this point, we calculated air/sea fluxes using these concentrations, and the expression $F = k_T*(C_w - C_a)H$, where $1/k_T = 1/Hk_a + 1/k_w$, and k_a and k_w are wind speed-based parameterizations of air-side and water-side gas transfer coefficients [*Kondo*, 1975; *Wanninkhof*, 1992].

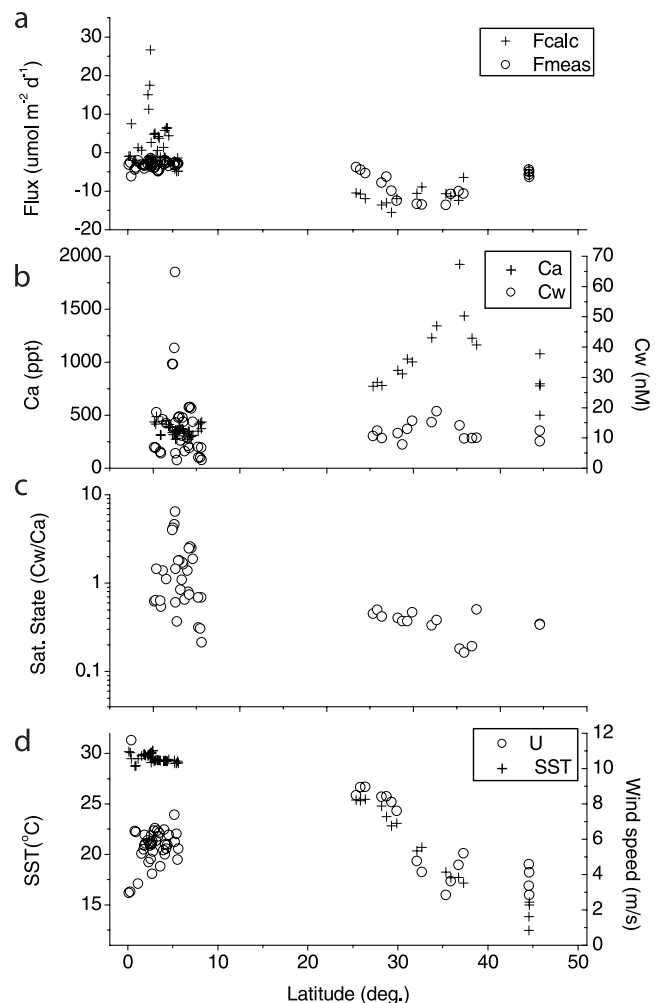


Figure 2. Shipboard measurements of acetone from the equatorial and North Pacific. From top: (a) Measured and calculated air/sea fluxes; (b) air and seawater acetone levels; (c) saturation state, expressed as C_w/C_a , where C_w is the measured seawater concentrations at 5m depth divided by the Henry's Law solubility [*Zhou and Mopper*, 1990]; and (d) sea surface temperature and mean wind speeds.

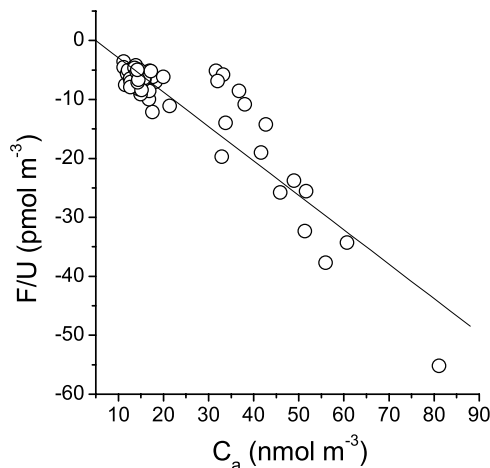


Figure 3. Relationship between air/sea flux of acetone, wind speed, and atmospheric acetone. The flux is scaled by wind speed (F/U) because wind speed based parameterizations [Kondo, 1975] suggest a linear relationship over the wind speed range encountered during this cruise.

These calculated fluxes will be called gradient fluxes in the remaining text. In the equatorial region, the mean gradient flux was $2.8 \pm 6.8 \mu\text{mol m}^{-2} \text{day}^{-1}$, with a range of -4.8 to $26.7 \mu\text{mol m}^{-2} \text{day}^{-1}$. Approximately half of the gradient fluxes were positive. In contrast, the fluxes measured by eddy covariance in this region had a mean of $-3.1 \pm 0.9 \mu\text{mol m}^{-2} \text{day}^{-1}$, ranging between -1.5 and $-6.2 \mu\text{mol m}^{-2} \text{day}^{-1}$. Just north of Hawaii, between 25 and 30°N , the gradient fluxes were all negative, i.e. into the ocean, in agreement with the eddy covariance fluxes. The magnitude of the gradient fluxes in this region, $-12.5 \pm 1.8 \mu\text{mol m}^{-2} \text{day}^{-1}$, was greater than the magnitude of the eddy covariance fluxes, $-7.2 \pm 3.2 \mu\text{mol m}^{-2} \text{day}^{-1}$. At latitudes above 30°N , there was good agreement between the two acetone fluxes, $-8.8 \pm 2.9 \mu\text{mol m}^{-2} \text{day}^{-1}$ and $-9.3 \pm 3.7 \mu\text{mol m}^{-2} \text{day}^{-1}$ respectively, with both indicating flux into the ocean surface. The air/sea fluxes of acetone were consistently larger in the mid latitudes than in the tropics, reflecting the higher atmospheric acetone levels and higher wind speeds.

[8] How can one reconcile the apparent inconsistency between the observed saturation states of the surface waters and the air/sea fluxes measured by eddy covariance? One possible explanation is that there are near surface gradients in acetone concentration, such that the concentration at 5m depth is not always representative of that at the sea surface. No measurements of the turnover rate of acetone in seawater have been made, but microbial uptake of acetone by aerobic bacteria has been demonstrated in culture [Nemecek-Marshall et al., 1995]. The only field study of acetone in the marine surface microlayer suggested that acetone should be elevated due to photochemical production, making the microlayer a strong source of atmospheric acetone [Zhou and Mopper, 1997]. The direction of the fluxes observed in this study and the lack of diel variability in seawater acetone measurements are not consistent with significant photochemical production in near surface waters. It should be noted that these previous studies employed different analytical techniques, which have not

been compared with our methods under field conditions [Kieber et al., 1990; Zhou and Mopper, 1997].

4. Implications for the Global Acetone Budget

[9] It is challenging to extrapolate these results globally. Simply scaling the average flux measured in this study to the entire ocean area yields a global ocean acetone sink of 33.2 Tg yr^{-1} . However, this does not account for latitudinal structure in atmospheric concentrations or sea surface winds. We find a strong relationship between the measured flux and the atmospheric concentration, as shown in Figure 3. The observed correlation suggests that either: 1) surface acetone levels are small compared to the atmospheric levels, and have little impact on the air/sea concentration gradient, or 2) surface acetone levels co-vary in some way with the atmospheric concentration, resulting in an air/sea gradient roughly proportional to C_a . The resulting relationship, $F/UC_a = 5.84 \times 10^{-4}$, is used as a basis for parameterizing the acetone flux in global models, with the caution that the processes underlying it are not fully understood. To make this calculation, we use COADS [Woodruff et al., 1993] monthly mean $1^\circ \times 1^\circ$ grid wind speed, temperature and pressure. We assume acetone levels in the marine boundary layer, ranging from 400 to 1000 ppt, based on this study and previously reported measurements [Jacob et al., 2002]. We calculate a global air-to-sea flux of $0.4 \text{ nmol m}^{-2} \text{day}^{-1}$ or 48 Tg yr^{-1} .

[10] An ocean sink of this magnitude would greatly imbalance the current atmospheric acetone budget [Jacob et al., 2002; Singh et al., 2004]. This imbalance is nearly offset by the recent reevaluation of the quantum yield for acetone photodissociation, suggesting that the atmospheric loss due to photolysis is considerably less than previously thought [Blitz et al., 2004]. We present an updated global budget for acetone in Table 1. The global acetone distribution was subdivided into boundary layer (900–1000 mbar) and free troposphere (100–900 mbar in tropics and 200–900 mbar elsewhere), for six months of summer and six months of winter, in large latitudinal bands ($40\text{--}90\text{N}$, $20\text{--}40\text{N}$, $0\text{--}20\text{N}$, $0\text{--}25\text{S}$, $25\text{--}90\text{S}$). Monthly average photolysis rates were calculated for 10° latitude bands with the Fast-J radiative transfer model [Wild et al., 2000] using absorption coefficients from Gierczak et al. [1998] and quantum yields from both Gierczak et al. [1998] and Blitz et al. [2004]. The global acetone loss due to reaction with OH was estimated using monthly mean, 8° latitude bands,

Table 1. Tropospheric Acetone Losses

	Jacob et al. [2002]	This Work
Burden, Tg	3.8	3.9
Sinks, Tg yr^{-1} :		
Ocean Deposition	14	48 ± 19^a
Land Deposition	9	9
Photolysis	46	24 ± 9^b
OH Reaction	27	20 ± 7
Total, Tg yr^{-1}	96	101 ± 66^c

^aUncertainties include OH, k_{OH} , σ_{aces} , Φ_{aces} , acetone distribution, U , and F/UC_a .

^bQuantum yields from Blitz et al. [2004]. Using Gierczak et al. [1998] quantum yields, the photolysis sink term is 54 Tg yr^{-1} .

^cThe acetone tropospheric lifetime is 0.039 yr (burden/total sinks).

OH and temperature fields [Spivakovsky *et al.*, 2000], and rate coefficients from Sander *et al.* [2003]. Using the revised quantum yields, we estimate a global loss rate of acetone by photolysis of 24 Tg yr⁻¹, roughly half of the previous rate. Summing all the calculated loss rates yields a global acetone loss rate of 101 Tg yr⁻¹, similar to the previous analysis, but with ocean uptake responsible for about half. Understanding this acetone ocean sink and its impact on atmospheric chemistry requires direct flux measurements with broader seasonal and spatial coverage, and insight into processes controlling oceanic acetone levels near the air/sea interface.

[11] **Acknowledgments.** Thanks to the OSU Marine Dept., D. Riemer, J. Edson, C. Friehe, F. Eisele, C. McCormick, M. Aydin, and I. Dioumaeva. This research was supported by ONR and NSF and is a contribution to the US SOLAS program.

References

- Apel, E. C., *et al.* (2003), A fast-GC/MS system to measure C₂ to C₄ carbonyls and methanol aboard aircraft, *J. Geophys. Res.*, *108*(D20), 8794, doi:10.1029/2002JD003199.
- Bandy, A. R., *et al.* (2002), Determination of the vertical flux of dimethyl sulfide by eddy correlation and atmospheric pressure ionization mass spectrometry (APIMS), *J. Geophys. Res.*, *107*(D24), 4743, doi:10.1029/2002JD002472.
- Blitz, M. A., D. E. Heard, and M. J. Pilling (2004), Pressure and temperature-dependent quantum yields for the photodissociation of acetone between 279 and 327.5 nm, *Geophys. Res. Lett.*, *31*, L06111, doi:10.1029/2003GL018793.
- Brasseur, G. P., *et al.* (1998), MOZART, a global chemical transport model for ozone and related chemical tracers: 1. Model description, *J. Geophys. Res.*, *103*, 28,265–28,289.
- Collins, W. J., *et al.* (1999), Role of convection in determining the budget of odd hydrogen in the upper troposphere, *J. Geophys. Res.*, *104*, 26,927–26,941.
- Edson, J. B., *et al.* (1998), Direct covariance flux estimates from mobile platforms at sea, *J. Atmos. Oceanic Technol.*, *15*, 547–562.
- Eisele, F. L. (1986), Identification of tropospheric ions, *J. Geophys. Res.*, *91*, 7897–7906.
- Gierczak, T., *et al.* (1998), Photochemistry of acetone under tropospheric conditions, *Chem. Phys.*, *231*, 229–244.
- Jacob, D. J., *et al.* (2002), Atmospheric budget of acetone, *J. Geophys. Res.*, *107*(D10), 4100, doi:10.1029/2001JD000694.
- Kaimal, J. C., *et al.* (1972), Spectral characteristics of surface-layer turbulence, *Q. J. R. Meteorol. Soc.*, *98*, 563–589.
- Kieber, R. J., X. Zhou, and K. Mopper (1990), Formation of carbonyl compounds from UV-induced photodegradation of humic substances in natural waters: Fate of riverine carbon in the sea, *Limnol. Oceanogr.*, *35*, 1503–1515.
- Kondo, J. (1975), Air-sea bulk transfer coefficients in diabatic conditions, *J. Boundary Layer Meteorol.*, *9*, 91–112.
- Lenschow, D. H. (1995), Micrometeorological techniques for measuring biosphere-atmosphere trace gas exchange, in *Biogenic Trace Gases: Measuring Emissions From Soil and Water*, edited by P. A. Matson, pp. 126, Blackwell Sci., Malden, Mass.
- Nemecek-Marshall, M., *et al.* (1995), Marine *Vibrio* species produce the volatile organic compound acetone, *Appl. Environ. Microbiol.*, *61*, 44–47.
- Sakai, R. K., D. R. Fitzjarrald, and K. E. Moore (2001), Importance of low-frequency contributions to eddy fluxes observed over rough surfaces, *J. Appl. Meteorol.*, *40*, 2178–2192.
- Sander, S. P., *et al.* (2003), Chemical kinetics and photochemical data for use in atmospheric studies, *Eval. 14, JPL Publ. 02–25*, Jet Propul. Lab., Pasadena, Calif.
- Shaw, W. J., C. W. Spicer, and D. V. Kenny (1998), Eddy correlation fluxes of trace gases using a tandem mass spectrometer, *Atmos. Environ.*, *32*, 2887–2898.
- Singh, H. B., *et al.* (1994), Acetone in the atmosphere: Distribution, sources, and sinks, *J. Geophys. Res.*, *99*, 1805–1819.
- Singh, H. B., M. Kanakidou, P. J. Crutzen, and D. J. Jacob (1995), High concentrations and photochemical fate of oxygenated hydrocarbons in the global troposphere, *Nature*, *378*, 50–54.
- Singh, H., *et al.* (2000), Distribution and fate of selected oxygenated organic species in the troposphere and lower stratosphere over the Atlantic, *J. Geophys. Res.*, *105*, 3795–3805.
- Singh, H., *et al.* (2001), Evidence from the Pacific troposphere for large global sources of oxygenated organic compounds, *Nature*, *410*, 1078–1081.
- Singh, H. B., A. Tabazadeh, M. J. Evans, B. D. Field, D. J. Jacob, G. Sachse, J. H. Crawford, R. Shetter, and W. H. Brune (2003), Oxygenated volatile organic chemicals in the oceans: Inferences and implications based on atmospheric observations and air-sea exchange models, *Geophys. Res. Lett.*, *30*(16), 1862, doi:10.1029/2003GL017933.
- Singh, H. B., *et al.* (2004), Analysis of the atmospheric distribution, sources, and sinks of oxygenated volatile organic chemicals based on measurements over the Pacific during TRACE-P, *J. Geophys. Res.*, *109*, D15S07, doi:10.1029/2003JD003883.
- Spivakovsky, C. M., *et al.* (2000), Three-dimensional climatological distribution of tropospheric OH: Update and evaluation, *J. Geophys. Res.*, *105*, 8931–8980.
- Viggiano, A. A., F. Dale, and J. F. Paulson (1988), Proton transfer reactions of H⁺(H₂O)_{n=2–11} with methanol, ammonia, pyridine, acetonitrile, and acetone, *J. Chem. Phys.*, *88*, 2469–2477.
- Wang, Y., D. J. Jacob, and J. A. Logan (1998), Global simulation of tropospheric O₃-NO_x-hydrocarbon chemistry: 1. Model formation, *J. Geophys. Res.*, *103*, 10,713–10,726.
- Wanninkhof, R. (1992), Relationship between wind speed and gas exchange over the ocean, *J. Geophys. Res.*, *97*, 7373–7382.
- Wennberg, P. O., *et al.* (1998), Hydrogen radicals, nitrogen radicals, and the production of O₃ in the upper troposphere, *Science*, *279*, 49–53.
- Wild, O., X. Zhu, and M. Prather (2000), Fast-J: Accurate simulations of in- and below-cloud photolysis in tropospheric chemistry models, *J. Atmos. Chem.*, *37*, 245–282.
- Williams, J., *et al.* (2000), Variability-lifetime relationship for organic trace gases: A novel aid to compound identification and estimation of HO concentrations, *J. Geophys. Res.*, *105*, 20,473–20,486.
- Williams, J., *et al.* (2001), An atmospheric chemistry interpretation of mass scans obtained from a proton transfer mass spectrometer flown over the tropical rainforest of Surinam, *J. Atmos. Chem.*, *38*, 133–166.
- Williams, J., *et al.* (2004), Measurements of organic species in air and seawater from the tropical Atlantic, *Geophys. Res. Lett.*, *31*, L23S06, doi:10.1029/2004GL020012.
- Woodruff, S. D., *et al.* (1993), Comprehensive Ocean-Atmosphere Data Set (COADS) release 1a: 1980–92, *Earth Syst. Monit.*, *4*, 1–8.
- Zhou, X., and K. Mopper (1990), Apparent partition coefficients of 15 carbonyl compounds between air and seawater and between air and freshwater; implications for air-sea exchange, *Environ. Sci. Technol.*, *24*, 1864–1869.
- Zhou, X., and K. Mopper (1997), Photochemical production of low-molecular-weight carbonyl compounds in seawater and surface microlayer and their air-sea exchange, *Mar. Chem.*, *56*, 201–213.

W. J. De Bruyn, Department of Physical Sciences, Chapman University, One University Drive, Orange, CA 92866, USA.

C. A. Marandino, S. D. Miller, M. J. Prather, and E. S. Saltzman, Department of Earth System Science, University of California, Irvine, 1212 Croul Hall, Irvine, CA 92697, USA. (cmarandi@uci.edu)